

Weyl Semimetal Type II classification.

Sabrina Rufo

Center of Physics and Engineering of Advanced Materials-
CeFEMA

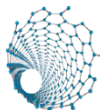
Beijing Computational Science Research Center - CSRC

November 18, 2021

QUANTUMMATTER
@PT



Quantum Agora



CeFEMA

Center of Physics and
Engineering of Advanced
Materials



CSRC




Overview

- Weyl semimetal WSMs.
- WSMs notable properties.
- Type-I and type-II WSMs classification.
- Transition Metal Dichalcogenide-TMDs
 WTe_2 and MoTe_2 .
- Janus-TMDs family \rightarrow topological classification.

Overview

- Weyl semimetal WSMs.
- WSMs notable properties.
- Type-I and type-II WSMs classification.
- Transition Metal Dichalcogenide-TMDs
WTe₂ and MoTe₂.
- Janus-TMDs family → topological classification.

WSM Type II



Nielsen-Ninomiya theorem

One Right-moving Fermion

On a Lattice: Crystals

Nielsen-Ninomiya theorem

One Right-moving Fermion

On a Lattice: Crystals

double fermion
left-moving state

Nielsen-Ninomiya theorem

One Right-moving Fermion

- Dimension?
- Symmetry?

On a Lattice: Crystals

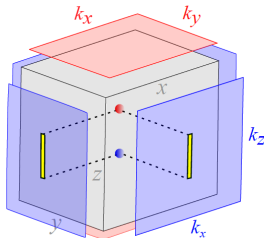
double fermion
left-moving state

Weyl Semimetal: notable properties

Broken symmetry mechanism

- Time-reversal symmetry-TRS.
 - Inversion Symmetry.
-
- Fermi arcs.
 - Chiral anomaly
 - negative magnetoresistance.

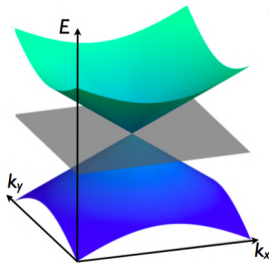
T-broken symmetry



Type I and type II Weyl semimetal

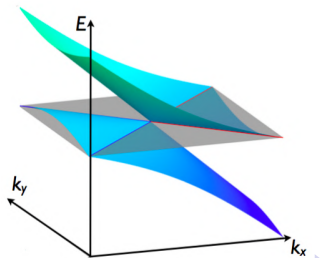
Type I WSM

- Weyl cones exhibit linear crossing bands.
- Lorentz symmetry.
- point-like Fermi surface cross-section.



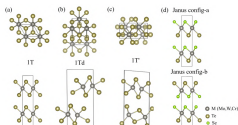
Type II WSM

- Weyl cones are tilted about the energy axis.
- Broken Lorentz symmetry.
- non-point-like Fermi surface cross-section.

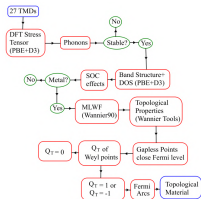


Transition Metal Dichalcogenides-TMDs WTe₂ and MoTe₂ → WSM Type II

Janus-TMDs



Workflow



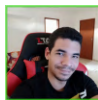
Enhancing topological Weyl Semimetals by Janus Transition Metal Dichalcogenides structures

M. A. R. Griffith^{*,†}, S. Rufo^{*,†}, A. C. Dias^{*,‡} and Juarez L. F. Da Silva^{*,¶}

[†]Beijing Computational Science Research Center, Building 9, East Zone, No.10 East Xibeiwang Road, Haidian District, Beijing 100193, China

[‡]CeFenna, Instituto Superior Técnico, Universidade de Lisboa, Av. Rovisco Pais, N° 1 1049-001 Lisboa, Portugal

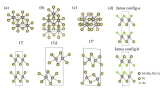
[¶]São Carlos Institute of Chemistry, University of São Paulo, PO Box 780, 13560 – 970, São Carlos, SP, Brazil



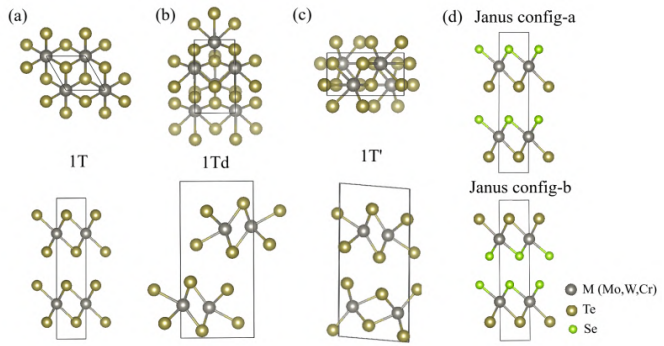
Transition Metal Dichalcogenides-TMDs WTe_2 and $MoTe_2$

$MoTe_2 \rightarrow$ WSM Type II

WSM Type II

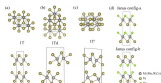


Workflow

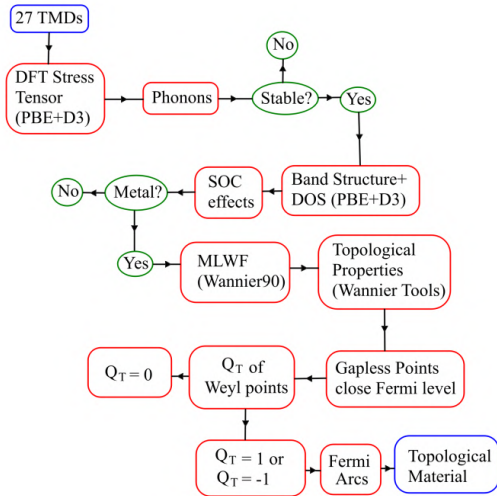


Transition Metal Dichalcogenides-TMDs WTe_2 and $MoTe_2 \rightarrow$ WSM Type II

WSM Type II

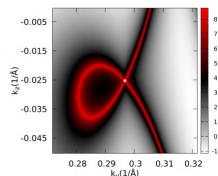
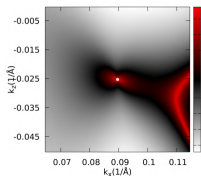
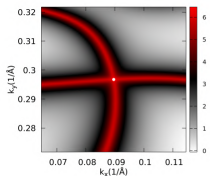
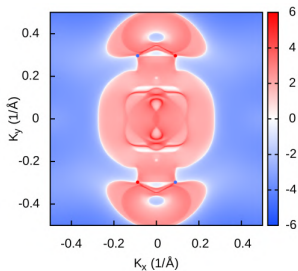


Workflow



3D Fermi Surface: WTeSe-XX $1T'$

Surface States



Janus-TMDs Topological classification

Type I - WTeSe-XX $1T_d$

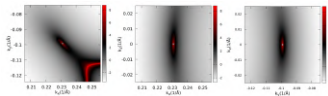
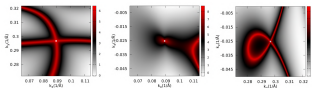


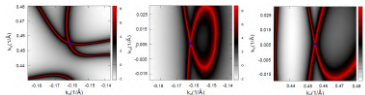
Table 3 Stable Janus topological classification.

Material	Topological Classification
WTeSe-XY- $1T_d$	strong Type II
WTeSe-XX- $1T'$	weak Type II
WTeSe-XX- $1T_d$	Type I
MoTeSe-XY- $1T_d$	strong Type II
MoTeSe-XX- $1T_d$	weak Type II
CrTeSe-XY- $1T'$	weak Type II
CrTeSe-XY- $1T_d$	strong Type II
CrTeSe-XX- $1T_d$	weak Type II

Weak Type II - WTeSe-XX $1T'$



Strong Type II - CrTeSe-XY $1T_d$



Difficults...

Fermi arcs and Weyl points

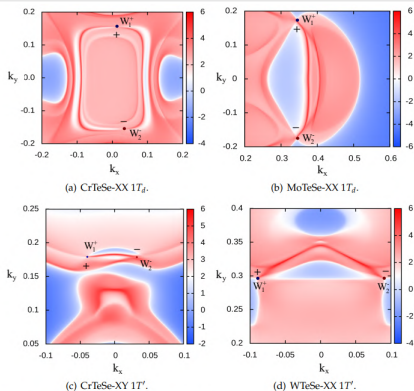
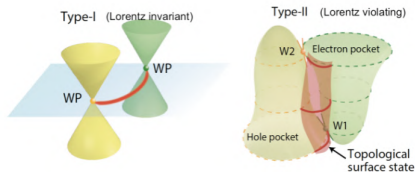


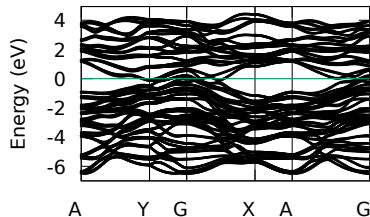
Figure 5 (Color online) Theoretical constant surface (001) energy contour plots for different compounds and energies. a) CrTeSe-XX $1T_d$ with $E = -3$ meV, b) MoTeSe-XX $1T_d$ with $E = -18$ meV. c) CrTeSe-XY $1T'$ with $E = -60$ meV and d) WTeSe-XX $1T'$ with $E = -18$ meV.

Type II Weyl semimetal

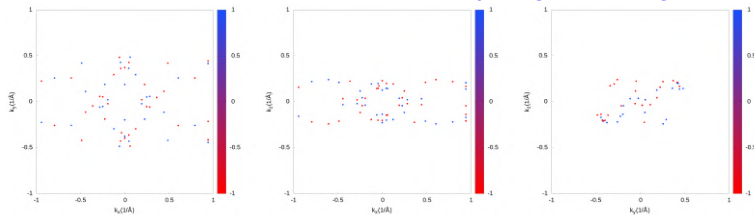


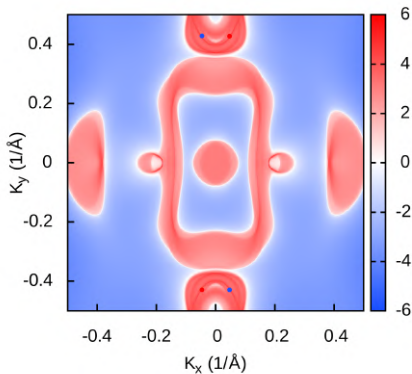
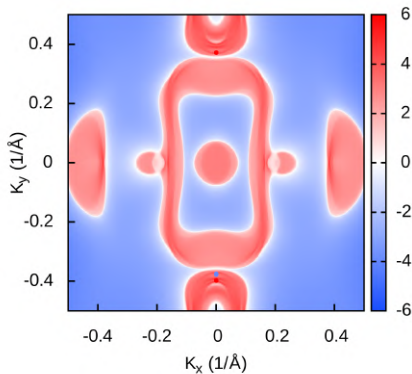
Protocol: MoTeSe-XY $1T_d$

Bulk bands



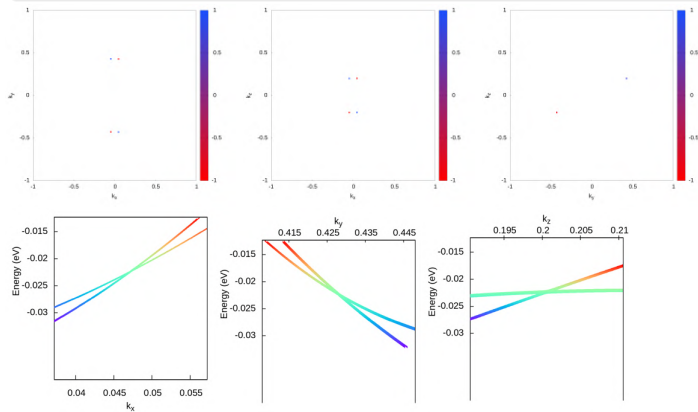
Topological charge



Protocol: MoTeSe-XY $1T_d$ candidate 1: $E=-0.0197\text{eV}$ candidate 2: $E=-0.0226\text{eV}$ 

Protocol: MoTeSe-XY $1T_d$

candidate 2: $E=-0.0226$; Weyls projection; Energy crossing



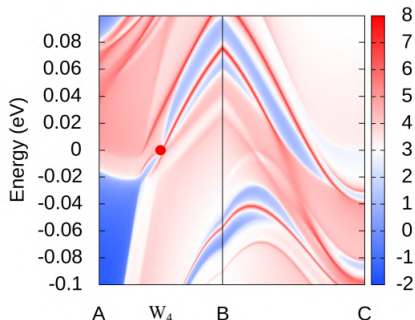
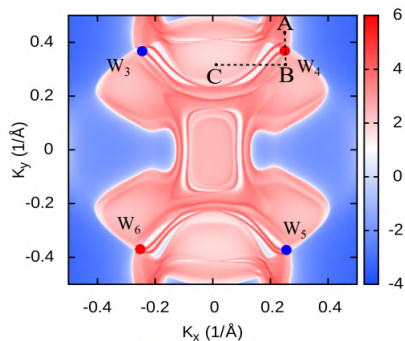
Janus-TMDs Topological classification

Topological charge and Weyl energies

Material	P. Group	$\vec{k}_{W_1^+} (\text{\AA}^{-1})$	$\vec{k}_{W_2^-} (\text{\AA}^{-1})$	$\Delta_k (\text{\AA}^{-1})$	$(E_{W_1^+}, E_{W_2^-})$ eV
WTe ₂ -1T _d	4[C _s]	(0.219,-0.045,0.000)	(0.219,0.045,0.000)	0.090	(0.056,0.056)
MoTe ₂ -1T _d	4[C _s]	(0.185,0.0539,0.000)	(0.187,-0.053,0.000)	0.100	(0.062,0.062)
WTeSe-XY-1T _d	4[C _s]	(-0.400,0.146,-0.072)	(-0.400,-0.145,0.072)	0.324	(-0.011,-0.012)
WTeSe-XX-1T'	4[C _s]	(-0.089,0.296,0.025)	(0.089,0.296,-0.025)	0.184	(-0.018,-0.018)
WTeSe-XX-1T _d	7[C _{2v}]	(0.231,-0.099,0.000)	(0.230,0.099,0.000)	0.139	(-0.016,-0.016)
MoTeSe-XY-1T _d	4[C _s]	(-0.047,0.429,0.200)	(0.047,0.428,0.200)	0.094	(-0.022,-0.022)
MoTeSe-XX-1T _d	7[C _{2v}]	(0.344,0.174,0.013)	(0.344,-0.174,-0.013)	0.348	(-0.045,0.045)
CrTeSe-XY-1T'	4[C _s]	(0.041,0.177,-0.030)	(-0.039,0.182,0.035)	0.103	(-0.060,-0.070)
CrTeSe-XY-1T _d	4[C _s]	(0.085,-0.501,-0.135)	(-0.053,-0.507,-0.162)	0.140	(-0.050,-0.058)
CrTeSe-XX-1T _d	7[C _{2v}]	(0.014,0.157, 0.218)	(0.034,-0.154,-0.231)	0.310	(-0.003, 0.001)
CrTeSe-XX-1T _d	7[C _{2v}]	(-0.245,0.369, -0.003)	(0.245,0.371,0.005)	0.490	(0.003,-0.001)

Janus-TMDs: CrTeSe – XX $1T_d$

Material	P. Group	$\vec{k}_{W_1^+} (\text{\AA}^{-1})$	$\vec{k}_{W_2^-} (\text{\AA}^{-1})$	$\Delta_k (\text{\AA}^{-1})$	$(E_{W_1^+}, E_{W_2^-})$ eV
CrTeSe – XX- $1T_d$	$7[C_{2v}]$	(-0.245, 0.369, -0.003)	(0.245, 0.371, 0.005)	0.490	(0.003, -0.001)



Review

Weyl semimetal

- Janus-TMDs.
- Topological classification.

Review

Weyl semimetal

- Janus-TMDs.
- Topological classification.

Thank you!



References



H. B. Nielsen and M. Ninomiya, The Adler-Bell-Jackiw anomaly and Weyl fermions in a crystal, Physics Letters B 130, (1983).



Jia, S., Xu, SY. Hasan, M. Weyl semimetals, Fermi arcs and chiral anomalies. Nature Mater 15, 1140–1144 (2016). <https://doi.org/10.1038/nmat4787>.



N.P. Armitage, E.J. Mele, and Ashvin Vishwanath. Weyl and Dirac semimetals in three-dimensional solids, Rev. Mod. Phys. 90, 015001 – (2018).



Wang, E., Lu, X., Ding, S. et al. Gaps induced by inversion symmetry breaking and second-generation Dirac cones in graphene/hexagonal boron nitride. Nature Phys 12, 1111–1115 (2016). <https://doi.org/10.1038/nphys3856>.



Lu, AY., Zhu, H., Xiao, J. et al. Janus monolayers of transition metal dichalcogenides. Nature Nanotech 12, 744–749 (2017). <https://doi.org/10.1038/nnano.2017.100>.



S. Rufo, M. A. R. Griffith, Nei Lopes et al. Anisotropic scaling in 3D topological models: from Weyl semimetal to Hopf insulator, 11 May 2021, PREPRINT (Version 1) available at Research Square [<https://doi.org/10.21203/rs.3.rs-515110/v1>].



website www.wanniertools.org.